Non-parametric Monitoring of Spatial Dependence

Philipp Adämmer

Institute of Data Science,
University of Greifswald

HELMUT SCHMIDT UNIVERSITÄT
Universität der Bundeswehr Hamburg

Philipp Wittenberg, Christian H. Weiß

Department of Mathematics & Statistics,
Helmut Schmidt University, Hamburg

MATH STAT

Murat C. Testik

Department of Industrial Engineering,
Hacettepe University Ankara

HELMUT SCHMIDT UNIVERSITÄT
Universität der Bundeswehr Hamburg

MATH STAT

Spatial Dependence in Rectangular Grid Data

Introduction

Spatial Dependence in Rectangular Grid Data

Real-valued and continuously distributed **spatial data** occurring in regular two-dimensional grid: $(Y_{\boldsymbol{s}})_{\boldsymbol{s}\in\mathbb{Z}^2}$.

(random field, spatial process in plane, regular lattice structure)

Data rectangles $(y_{\boldsymbol{s}}) = (y_{s_1,s_2})$ with $0 \leq s_1 \leq m$ and $0 \leq s_2 \leq n$.

Infer dependence in $(Y_{\boldsymbol{s}})$ via **spatial ordinal patterns** (SOPs), due to Ribeiro et al. (2012) and Bandt & Wittfeld (2023).

$d_1 \times d_2$-SOP computed from $d_1 \times d_2$-rectangle from $(y_{\boldsymbol{s}})$:

1. concatenate *rows* into vector of length $d_1 \cdot d_2$,
2. compute corresponding $(d_1 \cdot d_2)$th-order OP from $S_{d_1 \cdot d_2}$,
3. transform back into $d_1 \times d_2$-matrix in *row-wise* manner.

Definition of ordinal pattern (OP) in step 2 in usual way:

Entries of $\pi = (r_1, \ldots, r_d) \in S_d$ express

ranks within $\boldsymbol{y} = (y_1, \ldots, y_d) \in \mathbb{R}^d$, i. e.,

$$r_k < r_l \quad \Leftrightarrow \quad y_k < y_l \quad \text{or} \quad (y_k = y_l \text{ and } k < l)$$

for all $k, l \in \{1, \ldots, d\}$. Here, "$y_k = y_l$" if ties within $\boldsymbol{y}$.

As $|S_{d_1 \cdot d_2}| = (d_1 \cdot d_2)!$ quickly unfeasibly large,

Bandt & Wittfeld (2023) recommend focus on 2×2-**SOPs:**

$$\mathbf{Y}_s = \begin{pmatrix} Y_{s_1-1,s_2-1} & Y_{s_1-1,s_2} \\ Y_{s_1,s_2-1} & Y_{s_1,s_2} \end{pmatrix} =: \begin{pmatrix} y_1 & y_2 \\ y_3 & y_4 \end{pmatrix} \quad \mapsto \quad \begin{pmatrix} r_1 & r_2 \\ r_3 & r_4 \end{pmatrix},$$

where $(r_1, r_2, r_3, r_4) \in S_4$ is OP of (y_1, y_2, y_3, y_4).

Bandt & Wittfeld (2023): further partition into **types**,

$$\mathcal{S}_1 = \left\{ \begin{pmatrix} \mathbf{1} & 2 \\ 3 & 4 \end{pmatrix}, \begin{pmatrix} \mathbf{1} & 3 \\ 2 & 4 \end{pmatrix}, \begin{pmatrix} 2 & \mathbf{1} \\ 4 & 3 \end{pmatrix}, \begin{pmatrix} 2 & 4 \\ \mathbf{1} & 3 \end{pmatrix}, \begin{pmatrix} 3 & \mathbf{1} \\ 4 & 2 \end{pmatrix}, \begin{pmatrix} 3 & 4 \\ \mathbf{1} & 2 \end{pmatrix}, \begin{pmatrix} 4 & 2 \\ 3 & \mathbf{1} \end{pmatrix}, \begin{pmatrix} 4 & 3 \\ 2 & \mathbf{1} \end{pmatrix} \right\},$$

$$\mathcal{S}_2 = \left\{ \begin{pmatrix} 1 & \mathbf{2} \\ 4 & 3 \end{pmatrix}, \begin{pmatrix} 1 & 4 \\ \mathbf{2} & 3 \end{pmatrix}, \begin{pmatrix} \mathbf{2} & 1 \\ 3 & 4 \end{pmatrix}, \begin{pmatrix} \mathbf{2} & 3 \\ 1 & 4 \end{pmatrix}, \begin{pmatrix} 3 & \mathbf{2} \\ 4 & 1 \end{pmatrix}, \begin{pmatrix} 3 & 4 \\ \mathbf{2} & 1 \end{pmatrix}, \begin{pmatrix} 4 & 1 \\ 3 & \mathbf{2} \end{pmatrix}, \begin{pmatrix} 4 & 3 \\ 1 & \mathbf{2} \end{pmatrix} \right\},$$

$$\mathcal{S}_3 = \left\{ \begin{pmatrix} 1 & \mathbf{3} \\ 4 & 2 \end{pmatrix}, \begin{pmatrix} 1 & 4 \\ \mathbf{3} & 2 \end{pmatrix}, \begin{pmatrix} 2 & \mathbf{3} \\ 4 & 1 \end{pmatrix}, \begin{pmatrix} 2 & 4 \\ \mathbf{3} & 1 \end{pmatrix}, \begin{pmatrix} \mathbf{3} & 1 \\ 2 & 4 \end{pmatrix}, \begin{pmatrix} \mathbf{3} & 2 \\ 1 & 4 \end{pmatrix}, \begin{pmatrix} 4 & 1 \\ 2 & \mathbf{3} \end{pmatrix}, \begin{pmatrix} 4 & 2 \\ 1 & \mathbf{3} \end{pmatrix} \right\}$$

Formally: type of SOP equal to

that rank which shares a diagonal with rank 4.

Bandt & Wittfeld (2023): further partition into **types**,

$$\mathcal{S}_1 = \left\{ \begin{pmatrix} \mathbf{1} & 2 \\ 3 & 4 \end{pmatrix}, \begin{pmatrix} \mathbf{1} & 3 \\ 2 & 4 \end{pmatrix}, \begin{pmatrix} 2 & \mathbf{1} \\ 4 & 3 \end{pmatrix}, \begin{pmatrix} 2 & 4 \\ \mathbf{1} & 3 \end{pmatrix}, \begin{pmatrix} 3 & \mathbf{1} \\ 4 & 2 \end{pmatrix}, \begin{pmatrix} 3 & 4 \\ \mathbf{1} & 2 \end{pmatrix}, \begin{pmatrix} 4 & 2 \\ 3 & \mathbf{1} \end{pmatrix}, \begin{pmatrix} 4 & 3 \\ 2 & \mathbf{1} \end{pmatrix} \right\},$$

$$\mathcal{S}_2 = \left\{ \begin{pmatrix} 1 & \mathbf{2} \\ 4 & 3 \end{pmatrix}, \begin{pmatrix} 1 & 4 \\ \mathbf{2} & 3 \end{pmatrix}, \begin{pmatrix} \mathbf{2} & 1 \\ 3 & 4 \end{pmatrix}, \begin{pmatrix} \mathbf{2} & 3 \\ 1 & 4 \end{pmatrix}, \begin{pmatrix} 3 & \mathbf{2} \\ 4 & 1 \end{pmatrix}, \begin{pmatrix} 3 & 4 \\ \mathbf{2} & 1 \end{pmatrix}, \begin{pmatrix} 4 & 1 \\ 3 & \mathbf{2} \end{pmatrix}, \begin{pmatrix} 4 & 3 \\ 1 & \mathbf{2} \end{pmatrix} \right\},$$

$$\mathcal{S}_3 = \left\{ \begin{pmatrix} 1 & \mathbf{3} \\ 4 & 2 \end{pmatrix}, \begin{pmatrix} 1 & 4 \\ \mathbf{3} & 2 \end{pmatrix}, \begin{pmatrix} 2 & \mathbf{3} \\ 4 & 1 \end{pmatrix}, \begin{pmatrix} 2 & 4 \\ \mathbf{3} & 1 \end{pmatrix}, \begin{pmatrix} \mathbf{3} & 1 \\ 2 & 4 \end{pmatrix}, \begin{pmatrix} \mathbf{3} & 2 \\ 1 & 4 \end{pmatrix}, \begin{pmatrix} 4 & 1 \\ 2 & \mathbf{3} \end{pmatrix}, \begin{pmatrix} 4 & 2 \\ 1 & \mathbf{3} \end{pmatrix} \right\}$$

Visual representation of types by arrows along increasing rank:

$\mathcal{S}_1 =$ 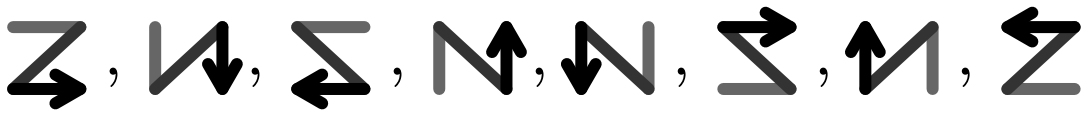 ("Z-type")

$\mathcal{S}_2 =$ 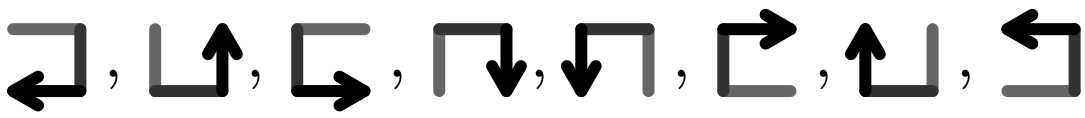 ("U-type")

$\mathcal{S}_3 =$ 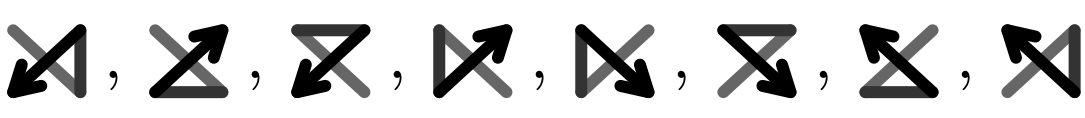 ("X-type")

Spatial Dependence in Rectangular Grid Data

If DGP is i. i. d., then type probabilities $\boldsymbol{p} = (\frac{1}{3}, \frac{1}{3}, \frac{1}{3})^\top$.

Bandt & Wittfeld (2023): statistics using type frequencies $\widehat{\boldsymbol{p}}$,

$$\widehat{\tau} = \widehat{p}_1 - 1/3 \quad \text{and} \quad \widehat{\kappa} = \widehat{p}_2 - \widehat{p}_3,$$
$$\widetilde{\tau} = \widehat{p}_3 - 1/3 \quad \text{and} \quad \widetilde{\kappa} = \widehat{p}_1 - \widehat{p}_2.$$

Weiß & Kim (2024) consider four **non-parametric tests for spatial dependence**, detailed **performance analyses**:

While spatial ACF superior for *linear unilateral* DGPs,

SOP-based tests often superior in presence of *outliers*,

for *non-linear* DGPs, and for *bilateral* spatial DGPs.

$\widetilde{\tau}$-test outperforms all other type-tests!

In present research, spatial dependence not in single data set, but **monitor streams of rectangular data**.

Various applications to quality control (monitoring of phone displays or textile images) and health surveillance, see Jiang et al. (2011), Megahed et al. (2012), Bui & Apley (2018), Tsiamyrtzis et al. (2022), and many more.

Outline:

- Novel EWMA-type control charts and performance analyses;
- three applications to climate data, war data, and quality data.
- **Work in progress:** monitoring higher-order dependence.

HELMUT SCHMIDT UNIVERSITÄT
Universität der Bundeswehr Hamburg

MATH STAT

Nonparametric Control Charts for Spatial Dependence

Definition & Competitor

Aim: monitor DGP $\left[(Y_{\boldsymbol{s}}^{(t)})_{\boldsymbol{s}}\right]_t$, where $t \in \mathbb{N}$ inspection time, and spatial locations $\boldsymbol{s} \in \{0,\ldots,m\} \times \{0,\ldots,n\}$.

If integer-valued RVs $X_{\boldsymbol{s}}^{(t)}$, then first transform to real-valued RVs $Y_{\boldsymbol{s}}^{(t)}$ by adding uniform noise:

$$Y_{\boldsymbol{s}} \;:=\; X_{\boldsymbol{s}} + U_{\boldsymbol{s}} \quad \text{with noise } (U_{\boldsymbol{s}})_{\mathbb{Z}^2} \text{ being i. i. d. U}(0,1).$$

General in-control (IC) assumption: rectangular sets $(Y_{\boldsymbol{s}}^{(t)})_{\boldsymbol{s}}$ independent for different t, but unique stationary random field.

True DGP out-of-control (OOC) if IC-model violated.

Particularly relevant special case:

(IC-iid) For each $t \in \mathbb{N}$, $(Y_{\boldsymbol{s}}^{(t)})_{\boldsymbol{s}}$ i. i. d. with continuous dist.

Here: SOPs and types for $\mathbf{Y}_{\boldsymbol{s}}^{(\boldsymbol{d})} = \begin{pmatrix} y_{s_1-d_1,s_2-d_2} & y_{s_1-d_1,s_2} \\ y_{s_1,s_2-d_2} & y_{s_1,s_2} \end{pmatrix}$ with **delay** $\boldsymbol{d} = \mathbf{1}$. Later, also larger delays $\boldsymbol{d} = (d_1, d_2)$.

Adapting Weiß & Testik (2023) for time-series monitoring, we use exponentially weighted moving average (EWMA) approach (Roberts, 1959) for "smoothed" type frequencies:

$$\widehat{\boldsymbol{p}}_0^{(\lambda)} \;=\; \boldsymbol{p}_0, \qquad \widehat{\boldsymbol{p}}_t^{(\lambda)} \;=\; \lambda\,\widehat{\boldsymbol{p}}_t + (1-\lambda)\,\widehat{\boldsymbol{p}}_{t-1}^{(\lambda)} \quad \text{for } t = 1, 2, \ldots$$

$\lambda = 1$ gives memory-less **Shewhart chart**,

$\lambda \in (0; 1)$ gives memory-type **EWMA chart**.

$\boldsymbol{p}_0$ from actual IC-model, e. g., $\boldsymbol{p}_0 = \left(\frac{1}{3}, \frac{1}{3}, \frac{1}{3}\right)^\top$ if "IC-iid".

EWMA charts with symmetric two-sided control limits (CLs):

$\widehat{\tau}$-chart: plot $\widehat{\tau}_t^{(\lambda)} = \widehat{p}_{t,1}^{(\lambda)} - \frac{1}{3}$, trigger alarm if $\left|\widehat{\tau}_t^{(\lambda)}\right| > l_{\widehat{\tau},\lambda}$;

$\widehat{\kappa}$-chart: plot $\widehat{\kappa}_t^{(\lambda)} = \widehat{p}_{t,2}^{(\lambda)} - \widehat{p}_{t,3}^{(\lambda)}$, trigger alarm if $\left|\widehat{\kappa}_t^{(\lambda)}\right| > l_{\widehat{\kappa},\lambda}$;

$\widetilde{\tau}$-chart: plot $\widetilde{\tau}_t^{(\lambda)} = \widehat{p}_{t,3}^{(\lambda)} - \frac{1}{3}$, trigger alarm if $\left|\widetilde{\tau}_t^{(\lambda)}\right| > l_{\widetilde{\tau},\lambda}$;

$\widetilde{\kappa}$-chart: plot $\widetilde{\kappa}_t^{(\lambda)} = \widehat{p}_{t,1}^{(\lambda)} - \widehat{p}_{t,2}^{(\lambda)}$, trigger alarm if $\left|\widetilde{\kappa}_t^{(\lambda)}\right| > l_{\widetilde{\kappa},\lambda}$.

Performance evaluation by (zero-state) average run length (ARL), i. e., mean number of plotted statistics until first alarm.

Chart design done by simulations (10^6 replications):

choose CLs such that ARL ≈ 370 under IC-conditions.

Special case "IC-iid": distribution of $(\hat{\boldsymbol{p}}_t)_t$ not depends on distribution of $Y_{\boldsymbol{s}}^{(t)} \Rightarrow$ **nonparametric/distribution-free** charts.

Possible (parametric!) competitor:

analogous EWMA chart based on spatial ACF.

Compute $\hat{\rho}(1)$ for each $(Y_{\boldsymbol{s}}^{(t)})_{\boldsymbol{s}}$,

apply EWMA smoothing to resulting sequence $(\hat{\rho}_t)$:

$$\hat{\rho}_0^{(\lambda)} = \rho_0, \qquad \hat{\rho}_t^{(\lambda)} = \lambda\,\hat{\rho}_t + (1-\lambda)\,\hat{\rho}_{t-1}^{(\lambda)} \quad \text{for } t = 1, 2, \ldots$$

Trigger alarm is at time t if $\left|\hat{\rho}_t^{(\lambda)}\right| > l_{\hat{\rho},\lambda}$.

Under "IC-iid", choose $\rho_0 = 0$, but still parametric!

HELMUT SCHMIDT UNIVERSITÄT
Universität der Bundeswehr Hamburg

MATH STAT

Nonparametric Control Charts for Spatial Dependence

Performance Analyses

Comprehensive simulation study with various IC- and OOC-DGPs, see Adämmer et al. (2025) for detailed results. Simulation study uses **Julia package** "OrdinalPatterns.jl", see subsequent talk by Philipp Adämmer ($\rightarrow$ GitHub).

Some **key findings** for illustration ("IC-iid"):

$\hat{\rho}$-EWMA chart erroneous IC-ARL if misspecified distribution,

m, n	t(2)	Exp	Poi	SkN	U	MixN	Ber
10, 10	590.76	464.82	410.59	389.60	357.43	352.20	349.14
15, 15	525.78	417.40	391.38	377.54	364.85	360.10	360.17
25, 25	457.68	389.41	380.83	374.69	368.64	365.42	366.65
40, 25	433.12	383.35	376.12	371.13	368.55	367.40	366.57

whereas nonparametric SOP charts always with ARL ≈ 370.

While $\widehat{\rho}$-chart superior for unilateral SAR(1, 1) process

$$Y_{t_1,t_2} = \alpha_1 \cdot Y_{t_1-1,t_2} + \alpha_2 \cdot Y_{t_1,t_2-1} + \alpha_3 \cdot Y_{t_1-1,t_2-1} + \varepsilon_{t_1,t_2}$$

with i. i. d. $\varepsilon_{t_1,t_2} \sim \mathrm{N}(0, 1)$, it deteriorates if additive outliers:

m, n	α_1	α_2	α_3	$\widehat{\tau}$-chart	$\widehat{\kappa}$-chart	$\widetilde{\tau}$-chart	$\widetilde{\kappa}$-chart	$\widehat{\rho}$-chart
10, 10	0.4	0.3	0.1	5.05	6.90	4.33	13.03	**2.47**
15, 15				3.27	4.29	2.86	7.57	**1.63**
25, 25				2.07	2.55	1.96	4.17	**1.0**
40, 25				1.81	2.09	1.56	3.26	**1.0**

vs.

m, n	α_1	α_2	α_3	AO	$\widehat{\tau}$-chart	$\widehat{\kappa}$-chart	$\widetilde{\tau}$-chart	$\widetilde{\kappa}$-chart	$\widehat{\rho}$-chart
10, 10	0.4	0.3	0.1	$\pm$10	9.85	8.74	**6.27**	57.94	41.13
15, 15					5.88	5.28	**3.95**	30.91	14.73
25, 25					3.35	3.06	**2.37**	14.05	6.34
40, 25					2.66	2.43	**2.01**	10.1	4.69

$\widetilde{\tau}$-chart also superior for bilateral SAR(1) DGP

$$Y_{t_1,t_2} = a_1 \cdot Y_{t_1-1,t_2} + a_2 \cdot Y_{t_1,t_2-1} + a_3 \cdot Y_{t_1,t_2+1} + a_4 \cdot Y_{t_1+1,t_2} + \varepsilon_{t_1,t_2},$$

both without outliers,

m, n	a_1	a_2	a_3	a_4	$\widehat{\tau}$-chart	$\widehat{\kappa}$-chart	$\widetilde{\tau}$-chart	$\widetilde{\kappa}$-chart	$\widehat{\rho}$-chart
10, 10	0.05	0.15	0.05	0.15	8.85	11.01	**6.87**	30.75	46.61
15, 15					5.35	6.41	**4.27**	16.36	15.31
25, 25					3.09	3.61	**2.55**	8.03	6.43
40, 25					2.46	2.85	**2.08**	6.0	4.73

and with outliers:

m, n	a_1	a_2	a_3	a_4	$\widehat{\tau}$-chart	$\widehat{\kappa}$-chart	$\widetilde{\tau}$-chart	$\widetilde{\kappa}$-chart	$\widehat{\rho}$-chart
10, 10	0.05	0.15	0.05	0.15	19.5	14.58	**10.47**	147.77	426.56
15, 15					10.68	8.19	**6.19**	91.35	141.25
25, 25					5.55	4.43	**3.49**	42.13	40.18
40, 25					4.25	3.46	**2.76**	28.94	24.73

Summary of general findings:

- $\tilde{\tau}$-EWMA chart universally applicable solution to uncover bilateral and nonlinear spatial dependence.
- While $\hat{\rho}$-chart superior for (clean!) unilateral DGPs, $\tilde{\tau}$-EWMA chart not much worse.
- By contrast to $\hat{\rho}$-chart, SOP charts nonparametric and robust, i. e., performance neither affected by actual IC-distribution nor by contamination with outliers.
- Same conclusions hold if considering integer-valued DGPs.

HELMUT SCHMIDT UNIVERSITÄT
Universität der Bundeswehr Hamburg

MATH STAT

Applications to Real-World Data Examples

Some Impressions

. . . for Tannenberg catchment (Aug 2007), $(m, n) = (26, 11)$.

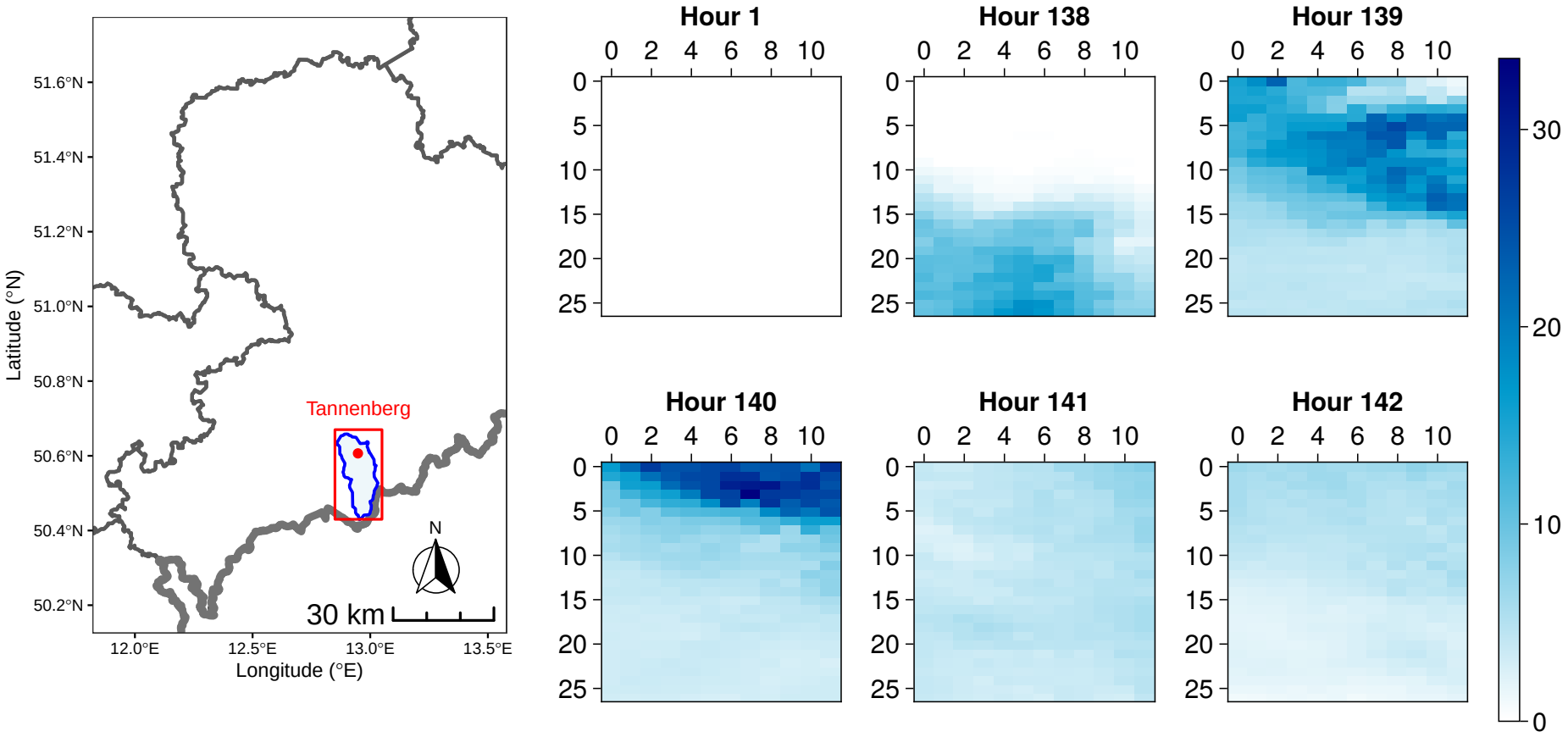

Data previously analyzed by Fischer et al. (2024).

$\tilde{\tau}$-EWMA chart with $\lambda = 0.1$:

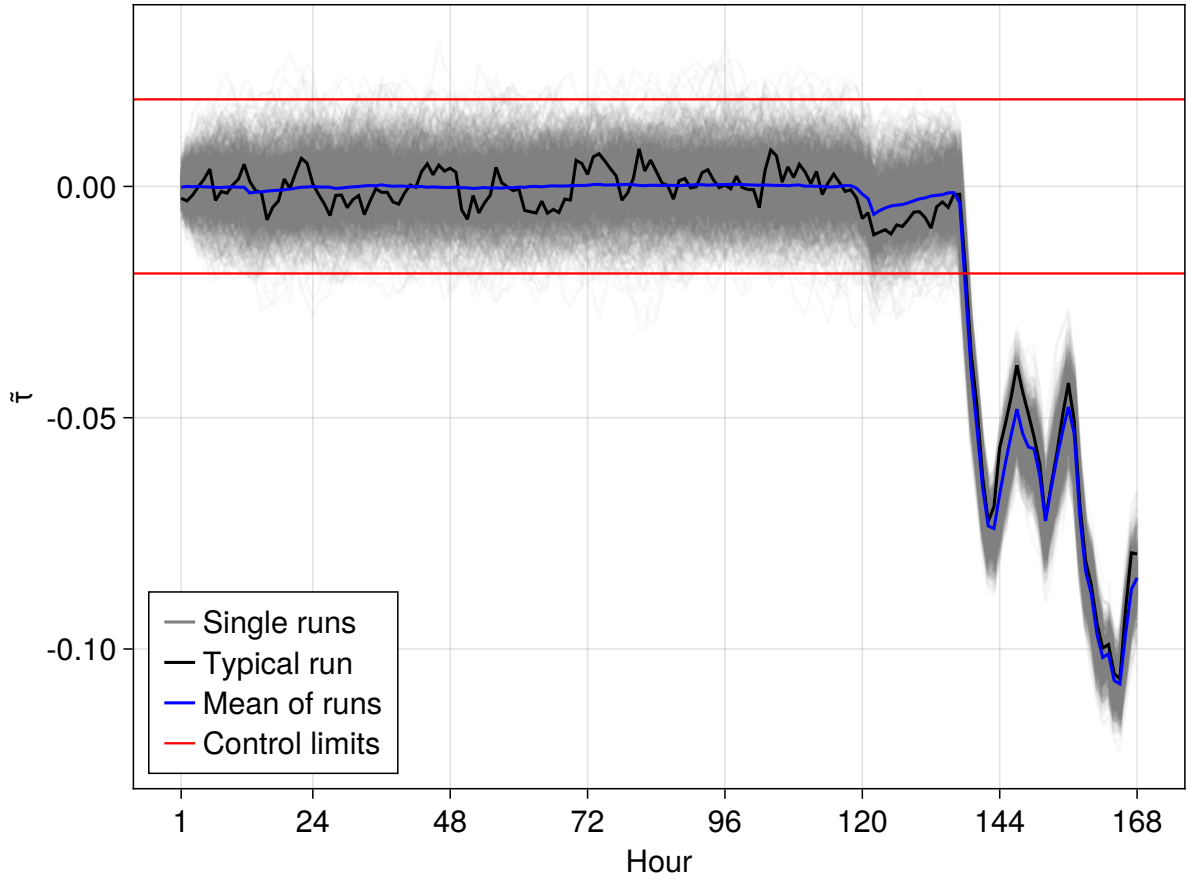

U(0, 0.1)-noise as measurement accuracy 0.1 mm.

Monitoring of War-related fires in Ukraine

Weekly numbers of war-related fires in 2023 and 2024 in eastern provinces of Ukraine (The Economist and S. Solstad):

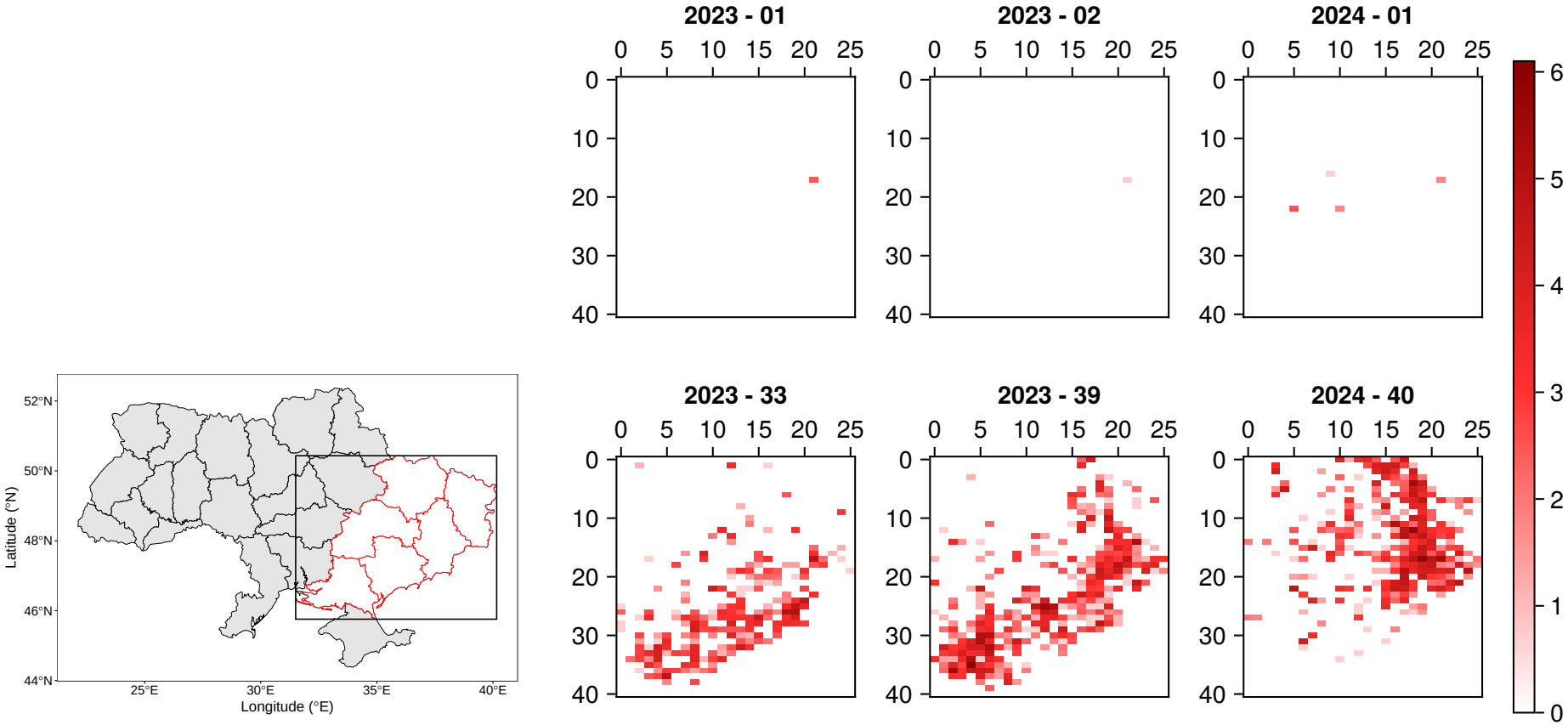

$\tilde{\tau}$-EWMA chart with $\lambda = 0.1$:

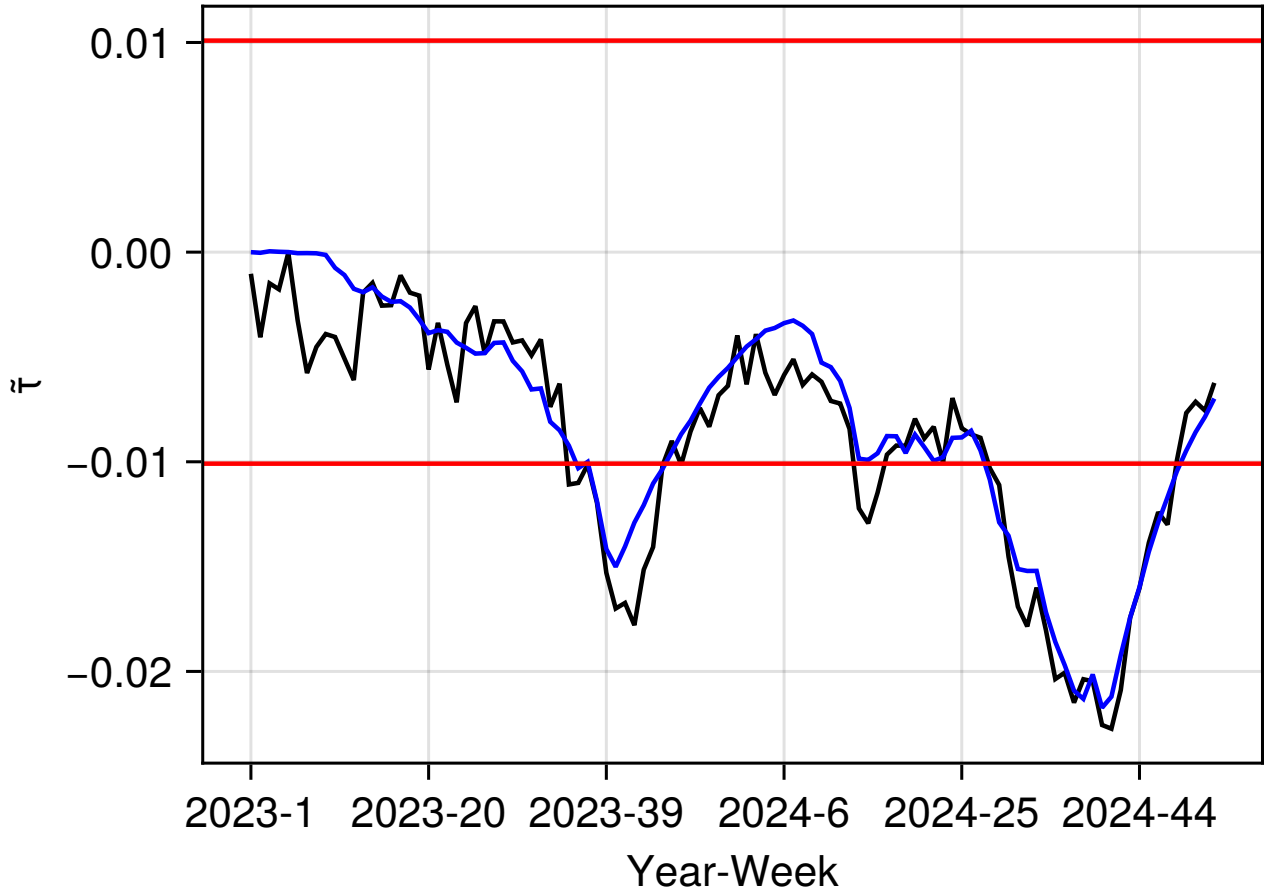

U(0, 1)-noise as discrete count data.

Monitoring Textile Images (Bui & Apley, 2018)

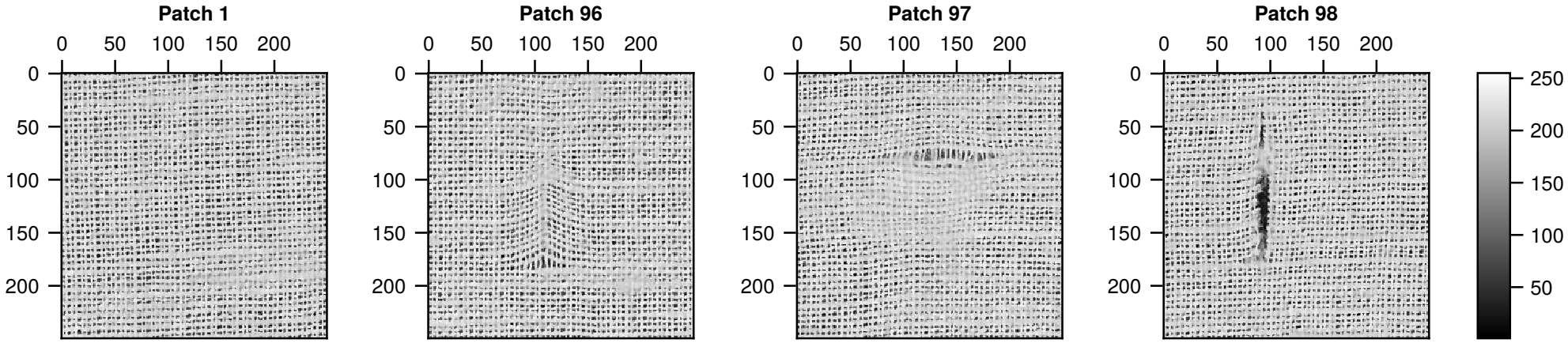

$\widetilde{\tau}$-EWMA charts with $\lambda = 0.1$:

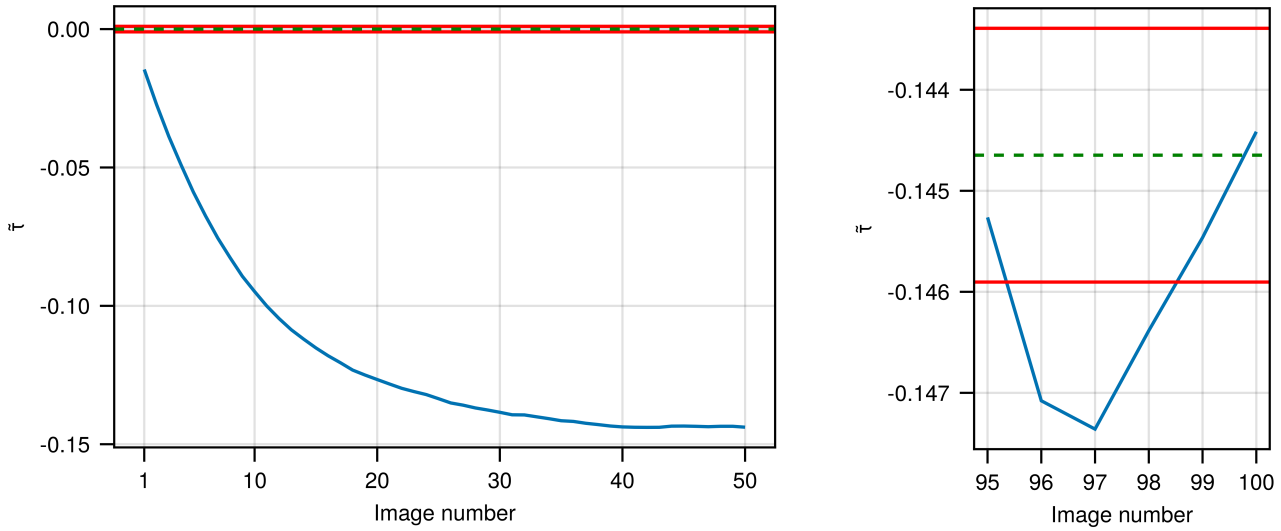

HELMUT SCHMIDT UNIVERSITÄT
Universität der Bundeswehr Hamburg

MATH STAT

Detecting Higher-Order Spatial Dependence

Work in Progress

Detecting Higher-Order Spatial Dependence

For previous control charts, SOPs calculated from directly neighboring observations (delay $\boldsymbol{d = 1}$), which is most important case as usually strongest dependence between adjacent observations (**first-order dependence**).

But maybe situations where dependence more pronounced for larger spatial lags (**higher-order dependence**), then SOPs with delay $d_1 + d_2 > 2$ more suitable.

If spatial dependencies weak but slowly decaying, then better consider **SOPs with multiple delays** at once.

Detecting Higher-Order Spatial Dependence

Let us focus on extensions of $\tilde{\tau}$-chart, which use "$\boldsymbol{d}$-SOPs" and "$\boldsymbol{d}$-types" from $\mathbf{Y}_{\boldsymbol{s}}^{(\boldsymbol{d})} = \begin{pmatrix} y_{s_1-d_1,s_2-d_2} & y_{s_1-d_1,s_2} \\ y_{s_1,s_2-d_2} & y_{s_1,s_2} \end{pmatrix}$ with delay $\boldsymbol{d} = (d_1, d_2) \in \mathbb{N}^2$ and $d_1 + d_2 > 2$.

EWMA approach adapted to **delay $\boldsymbol{d}$** by

$$\widehat{\boldsymbol{p}}_0^{(\lambda,\boldsymbol{d})} = \boldsymbol{p}_0^{(\boldsymbol{d})}, \qquad \widehat{\boldsymbol{p}}_t^{(\lambda,\boldsymbol{d})} = \lambda\, \widehat{\boldsymbol{p}}_t^{(\boldsymbol{d})} + (1-\lambda)\, \widehat{\boldsymbol{p}}_{t-1}^{(\lambda,\boldsymbol{d})} \quad \text{for } t = 1, 2, \ldots,$$

where $\widehat{\boldsymbol{p}}_t^{(\boldsymbol{d})}$ frequency vector of $\boldsymbol{d}$-types.

Under "IC-iid", one chooses $\boldsymbol{p}_0^{(\boldsymbol{d})} = (\frac{1}{3}, \frac{1}{3}, \frac{1}{3})^\top$. Then $\tilde{\tau}^{(\boldsymbol{d})}$-chart:

$$\text{plot } \tilde{\tau}_t^{(\lambda,\boldsymbol{d})} = \hat{p}_{t,3}^{(\lambda,\boldsymbol{d})} - \tfrac{1}{3}, \quad \text{trigger alarm if } \left|\tilde{\tau}_t^{(\lambda,\boldsymbol{d})}\right| > l_{\tilde{\tau},\lambda,\boldsymbol{d}}.$$

Detecting Higher-Order Spatial Dependence

If we want to aggregate information for several delays $\boldsymbol{d}$, we propose **Box–Pierce approach**, inspired by Bui & Apley (2018), where for "window size" $w \in \mathbb{N}$, we define $\tilde{\tau}^{\mathrm{BP}(w)}$-EWMA chart via

$$\tilde{\tau}_t^{\mathrm{BP}(\lambda,w)} = \sum_{d_1,d_2=1}^{w} \left(\tilde{\tau}_t^{(\lambda,\boldsymbol{d})} - \tilde{\tau}_0^{(\boldsymbol{d})}\right)^2.$$

IC-value $\tilde{\tau}_0^{(\boldsymbol{d})}$ equal to zero under assumption "IC-iid".

Performance analyses quite promising so far, so for **future research**, try BP-approaches also in other OP-areas, e. g., classical hypothesis tests for serial or spatial dependence.

Thank You for Your Interest!

MATH
STAT

Christian H. Weiß

Department of Mathematics & Statistics

Helmut Schmidt University, Hamburg

weissc@hsu-hh.de

Literature

Adämmer et al. (2025) Non-parametric monitoring of spatial dependence. *arXiv preprint* 2408.17022.

Bandt & Wittfeld (2023) Two new parameters ... *Chaos* **33**, 043124.

Bui & Apley (2018) A monitoring and diagnostic ... *Technomet* **60**, 1–13.

Fischer et al. (2024) Multivariate motion ... *SERRA* **38**, 1235–1249.

Jiang et al. (2011) Spatiotemporal surveillance ... *Stat Med* **30**, 569–583.

Megahed et al. (2012) A spatiotemporal method ... *QREI* **28**, 967–980.

Ribeiro et al. (2012) Complexity-entropy ... *PLoS ONE* **7**, e40689.

Roberts (1959) Control chart tests ... *Technomet* **1**, 239–250.

Tsiamyrtzis et al. (2022) Image based statistical ... *QE* **34**, 96–124.

Weiß & Kim (2024) Using spatial ordinal ... *Spat Stat* **59**, 100800.

Weiß & Testik (2023) Non-param. control ch... *Technomet* **65**, 340–350.